Note

Structural Basis for Targeting the Folded P-Loop Conformation of c-MET

Gavin W. Collie,*,[||] Iacovos N. Michaelides,[||] Kevin Embrey, Christopher J. Stubbs, Ulf Börjesson, Ian L. Dale, Arjan Snijder, Louise Barlind, Kun Song, Puneet Khurana, Christopher Phillips, and R. Ian Storer

Cite This: *ACS Med. Chem. Lett.* 2021, 12, 162−167

Read Online

ACCESS | Metrics & More | Article Recommendations | SI Supporting Information

ABSTRACT: We report here a fragment screen directed toward the c-MET kinase from which we discovered a series of inhibitors able to bind to a rare conformation of the protein in which the P-loop adopts a collapsed, or folded, arrangement. Preliminary SAR exploration led to an inhibitor (7) with nanomolar biochemical activity against c-MET and promising cell activity and kinase selectivity. These findings increase our structural understanding of the folded P-loop conformation of c-MET and provide a sound structural and chemical basis for further investigation of this underexplored yet potentially therapeutically exploitable conformational state.

KEYWORDS: *c-MET, kinase, X-ray crystallography, P-loop, small molecule inhibitor*
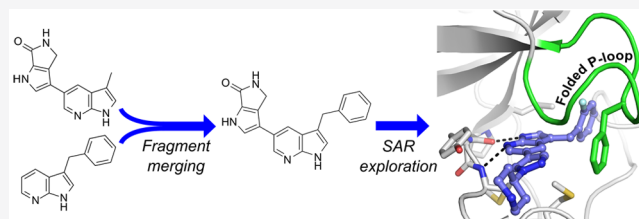
Kinases have received considerable attention over the past 20 years as drug targets, particularly in the area of oncology, with around 50 small molecule drugs approved to date.[5,6] Structure-based methods such as X-ray crystallography have played a key role in the discovery of many of these drugs and have enabled the characterization of a number of distinct kinase conformations. Interestingly, the targeting of a specific conformational state of a kinase is frequently associated with a specific (and often favorable) activity profile. For example, it has been shown that displacing either the αC-helix or a conserved DFG motif within the activation loop (A-loop) can lead to inhibitors with favorable selectivity, affinity, and/or kinetic properties.[7−12] In addition, some kinases have been seen to adopt a conformation in which the P-loop ("phosphate-binding" loop, also referred to as the "glycine-rich" loop) is collapsed into the ATP binding site, referred to from hereon as the "folded P-loop" conformation. Although rare (only identified in approximately 10 kinases to date[13−15]), there is good evidence to suggest that targeting the folded P-loop conformation could be a potential route to improving both the selectivity and potency of kinase inhibitors.[14,16]

The receptor tyrosine kinase c-MET[17] is among the few kinases reported to adopt a folded P-loop conformation, evident in the crystal structure of the apo autoinhibited form of the protein[2] (Figure 1). c-MET has attracted considerable attention as an anticancer drug target, with a significant number of small molecules having been assessed in clinical trials.[18] As with many other disease-relevant kinases, most c-MET-targeted inhibitors fall into one of three categories based on their binding mode: type-I, type-1.5 or type-II. Type-I
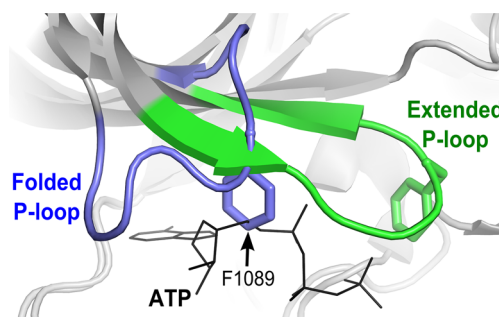
Figure 1. c-MET P-loop conformations.[1] Blue: "folded" P-loop seen in the apo autoinhibited form of the kinase (PDB Id 2G15).[2] Green: extended conformation seen in active ATP-bound structure (PDB Id 3DKC).[3]

inhibitors of c-MET, such as crizotinib,[19] localize to the ATP-binding site and typically exploit interactions with key A-loop residues to achieve high selectivity, yet have been shown to suffer from the emergence of acquired resistance in the clinic.[20−24] Type-1.5 and type-II c-MET inhibitors also bind to the ATP-binding site but in addition extend into the kinase
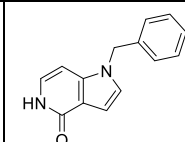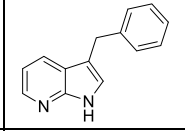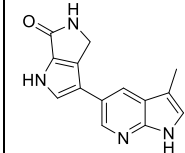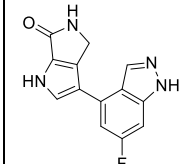
back-pocket. Such inhibitors are often highly potent yet are typically less selective than type-I c-MET inhibitors,[25] which may limit their clinical application. In addition, the molecular weight of type-1.5 and type-II compounds, often needing to be greater than 500 Da to drive sufficient potency and selectivity,[18] can pose significant challenges for oral bioavailability.

Despite the significant number of c-MET-targeted small molecule inhibitors that have been reported, where structural data is available, almost all bind to the kinase with the P-loop in the "extended" or "active" conformation (Figure 1). To our knowledge, there is just one chemical series reported shown to target c-MET with a folded P-loop,[4] and interestingly, the inhibitors reported by D'Angelo and co-workers, which belong to the type-1.5 inhibitor class, display both favorable potency and selectivity for c-MET. Targeting the folded P-loop conformation of c-MET could therefore be of potential therapeutic utility, and in particular, the exploration of alternative inhibitor classes (e.g., type-I or II) to target this conformational state of c-MET could provide alternative routes to inhibiting this kinase. In this vein, we report herein a fragment-based screening campaign directed toward c-MET from which we discovered a number of fragments shown by crystallography to bind to the folded P-loop conformation of the kinase. Structure-guided merging of two of these fragments followed by preliminary SAR exploration led to an inhibitor with nanomolar biochemical activity and promising cell activity and kinase selectivity. These results potentially offer a novel route to targeting c-MET as well as a structural framework to guide further investigations.

With the aim of discovering novel small molecule inhibitors of c-MET, we screened a library of 1150 fragments against the isolated kinase domain of wild-type human c-MET using ligand-observed 1D NMR (for full details of methods, see the Supporting Information). The screen yielded a hit rate of around 6%, with fragment hits analyzed by SPR to confirm binding to c-MET and determine affinities. Around 20 fragments were identified as positive binders by SPR, the majority of which we attempted to cocrystallize with the kinase domain of c-MET.[26] The majority of these experiments yielded no or poorly diffracting crystals; however, a 1.75 Å cocrystal structure was determined for compound 1 (Table 1). To our surprise, this revealed the compound to bind to the hinge region of the kinase with the P-loop in the collapsed/folded conformation (Figure 2a), highly similar to that seen in the previously reported apo autoinhibited crystal structure of c-MET[2] (Figure 2a, inset). Compound 1 binds to the hinge residues P1158 and M1160 via its pyridone nitrogen and carbonyl groups, with the benzyl ring orientated toward the non-displaced DFG motif (Figure 2a). The conformation of the P-loop, as seen here, creates a highly enclosed hydrophobic ligand binding site, in which the conserved aromatic residue of the c-MET P-loop, F1089, packs tightly against the fragment.

Comparison of the crystal structure of compound 1 bound to c-MET with the folded P-loop ligand complex reported by D'Angelo and co-workers[4] reveals distinct differences, particularly with respect to the conformations of the A-loop and P-loop (Figure 2b). Compound 1 adopts a type-I binding mode, anchored to the hinge via hydrogen bonds, with the benzyl group packing up against a β-turn motif formed from residues F1223-R1227 of the A-loop (Figure 2a and b). Interestingly, the conformation of this β-turn motif and the emergent A-loop effectively separates three key catalytic

**Table 1. Summary of Affinity and Activity Data of Compounds 1−4 for c-MET**

Cmpd	Structure	K_D / μM[b]	IC$_{50}$ / μM[c]
1[a]		> 100	NT
2		97.0 (17.1)	24.2 (5.3)
3		5.1 (0.4)	2.9 (2.4)
4		8.0 (0.4)	9.6 (1.0)

[a]Details of NMR and SPR characterization of compound 1 can be found in Figure S3. [b]SPR-derived dissociation constants (K_Ds). For further details, see Figures S3 and S4. [c]ADP-Glo biochemical enzyme inhibition assay. "NT": not tested. K_D and IC$_{50}$ values are the average of at least three separate experiments with standard deviation shown in brackets. For full details see the Supporting Information.

residues: K1110, E1127, and D1222 (Figure S2a). In this respect, in addition to the conformation of the P-loop (Figure 2a, inset), the c-MET-compound 1 structure closely resembles that of the apo autoinhibited protein.[2] In contrast, the type-1.5 compound reported by D'Angelo and co-workers displaces this β-turn motif (Figure 2b), with the conformation of the P-loop, although collapsed, differing noticeably to that of the apo autoinhibited kinase (Figures 2b and S2b). Consequently, by binding to the folded P-loop conformation of c-MET, yet with a type-I binding mode involving key structural features of the autoinhibited kinase, compound 1 appears to represent a novel mode of targeting c-MET. Due to this, plus the rarity of folded P-loops in general and their link with selectivity and potency,[14,16] we decided to explore this binding mode further. A 2D similarity search of the AstraZeneca internal chemical library was carried out for analogues of compound 1, with selected compounds tested by SPR and in a biochemical enzyme-inhibition assay.[27] This led to the identification of compound 2 (Table 1), with K_D and IC$_{50}$ values for c-MET of 97.0 and 24.2 μM, respectively. Compound 2 was also cocrystallized with c-MET, with the structure revealing the compound to bind to the kinase with a folded P-loop, involving key hydrogen bonding interactions from the 7-azaindole nitrogen atoms to the hinge region (residues P1158 and M1160), and the benzyl ring buried deep in the binding pocket (Figure 2c).

Comparison of the compound 1- and compound 2-c-MET structures reveals near perfect alignment of the P-loops (Figure S2c), yet there were nevertheless clear differences in hinge interactions and ligand geometry between the two binding
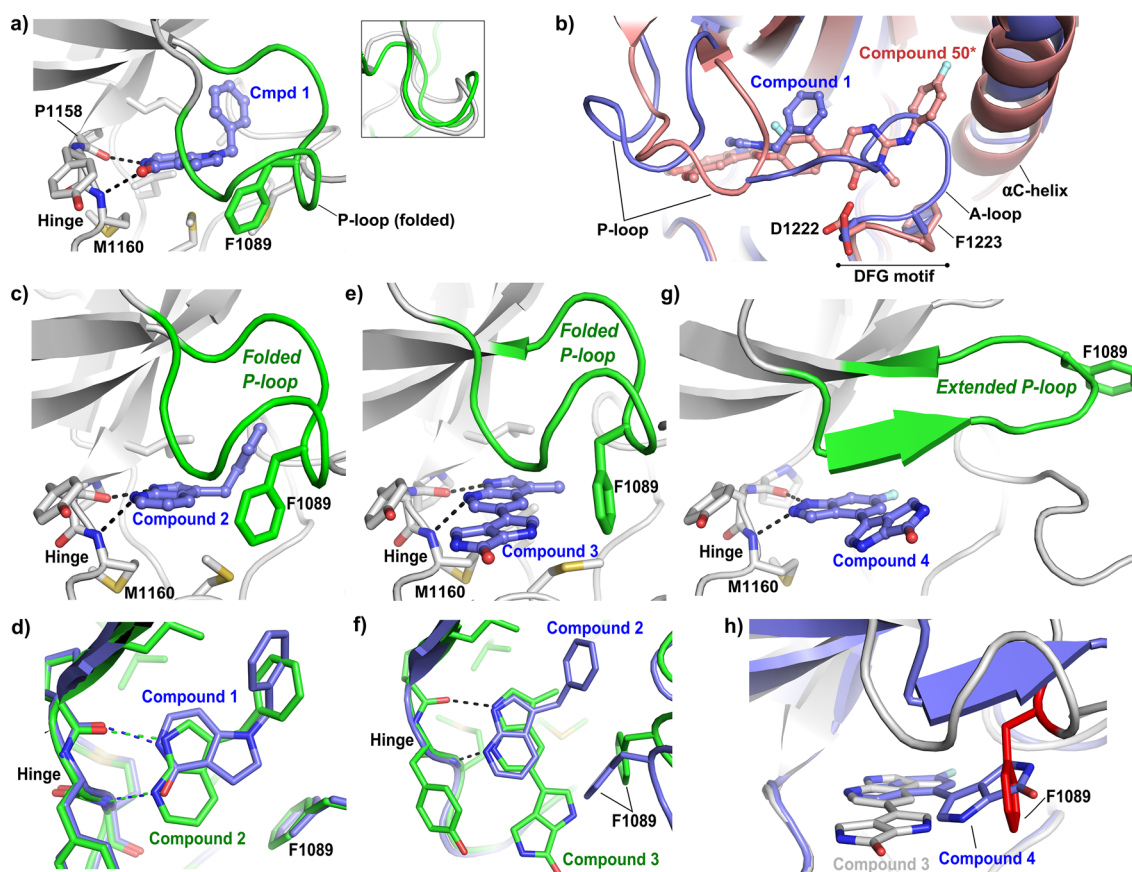
Figure 2. (a) Crystal structure of c-MET bound by compound **1** with a folded P-loop (highlighted green). Inset: structural alignment of the P-loop from the c-MET-compound **1** complex (green) with the P-loop from the apo autoinhibited kinase (white).[2] (b) Comparison of the binding modes of compound **1** (blue) versus compound **50** (pink) reported by D'Angelo et al.[4] for c-MET. *Compound and numbering from D'Angelo et al., 2008.[4] (c) Crystal structure of c-MET bound by compound **2** (P-loop highlighted green). (d) Overlay of c-MET-compound-**1** (blue) vs c-MET-compound **2** (green) crystal structures. (e) Crystal structure of compound **3** bound to c-MET (P-loop in green). (f) Comparison of c-MET-compound **2** (blue) vs c-MET-compound **3** (green) crystal structures. (g) Crystal structure of compound **4** bound to c-MET (P-loop in green). (h) Comparison of c-MET-compound **3** (white) vs c-MET-compound **4** (blue) crystal structures. F1089 of c-MET-compound **3** complex highlighted red. Structures in panels (c), (e), and (g) are in the same orientation, aligned to the structure in (c). Crystallographic data processing and refinement statistics for all crystal structures reported in this work can be found in Table S1.

modes (Figures 2d and S2c), which led us to undertake a second search of our internal chemical library for analogues, this time using compound **2** as a search template. Selected analogues of compound **2** were tested by SPR and biochemically, which revealed two stand-out hits: compound **3**, with K_D and IC_{50} values of 5.1 and 2.9 μM, respectively, and compound **4**, with K_D and IC_{50} values of 8.0 and 9.6 μM, respectively (Table 1). Cocrystallization of these compounds with c-MET revealed compound **3** to bind to the folded P-loop conformation of the kinase (Figure 2e), with the 7-azaindole group binding to the hinge region, overlaying very closely with the equivalent region of compound **2** in complex with c-MET (Figure 2f). The pyrrolopyrrolinone group of compound **3**, which is directed toward the solvent, packs against F1089, the position of which is slightly shifted relative to its position in the equivalent compound **2** complex (Figures 2f and S2d). In contrast, the crystal structure of c-MET bound by compound **4** revealed this molecule to adopt a surprising canonical hinge binding mode, with the fluoro indazole group bound to the hinge region and the P-loop in an "extended" conformation (Figure 2g). Structural alignment of the compound **3**- and compound **4**-c-MET complexes provided a clear explanation for the binding mode of compound **4** — with the fluoro-

indazole group of compound **4** bound to the hinge region, the pyrrolopyrrolinone moiety would severely clash with F1089 if it were to adopt the position it does in the folded P-loop conformation. (Figure 2h).

Comparison of the cocrystal structures of compound **2** and compound **3** bound to c-MET showed the 7-azaindole moieties of both compounds to adopt very similar positions (Figure 2f), which led us to attempt a structure-guided merging approach in an attempt to improve potency. Compound **5**, a hybrid of compounds **2** and **3**, was designed and synthesized, with subsequent enzyme inhibition giving an IC_{50} value of 660 nM[28] (Table 2). Compound **5** was also cocrystallized with c-MET, which pleasingly revealed a folded P-loop binding mode (Figure 3a), with the position of the hybrid (**5**) overlaying very closely with the pre-merged individual fragments (Figure S2e).

A search of our internal chemical library was then carried out in order to identify structurally similar analogues of compound **5** in an attempt to improve both potency and physicochemical properties. The crystal structure of c-MET bound by compound **5** (Figure 3a) strongly suggested that modification of the pyrrolopyrrolinone group, which is directed toward solvent, may allow us to modulate solubility and lipophilicity

Table 2. Biochemical and Cellular Activity of Compounds 5−9 for c-MET

Cmpd	Structure	LogD[a]	IC$_{50}$ / nM *Biochemical*[b]	LE[c]	LLE[d]	IC$_{50}$ / μM *Cell HTRF*[e]
5		4.0	660 (250)	0.34	2.18	21.88 (6.14)
6		2.31	48 (28)	0.37	5.01	5.94 (0.63)
7		2.50	44 (23)	0.36	4.86	1.88 (0.72)
8		2.40	65 (23)	0.35	4.79	3.12 (0.80)
9		2.40	137 (47)	0.34	4.46	4.71 (0.56)

[a]LogD measured via shake-flask method in octanol and water at pH 7.4. [b]ADP-Glo biochemical enzyme inhibition assay performed as in Table 1. [c]LE (ligand efficiency) = $1.37(\text{pIC}_{50}/\text{heavy atoms})$ with units of kcal mol^{-1} per heavy atom. [d]LLE (ligand-lipophilicity efficiency) = pIC_{50} − logD. [e]Cellular homogeneous time-resolved FRET assay. Details can be found in the Supporting Information. All IC$_{50}$ values are the average of at least three experiments with standard deviation shown in brackets.
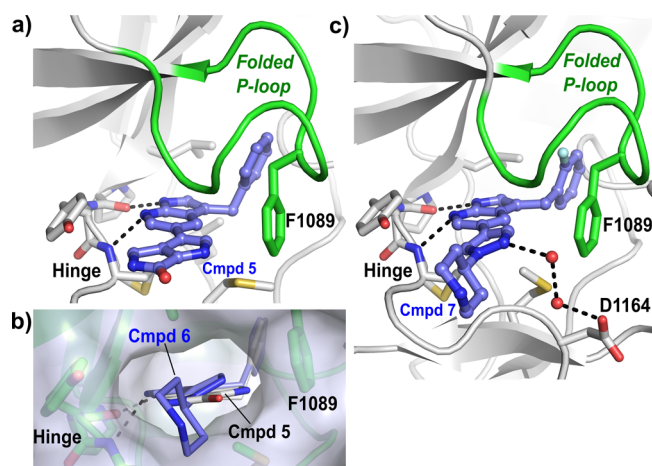
Figure 3. (a) Crystal structure of c-MET bound by compound **5**. (b) Comparison of compound **5**- vs compound **6**-c-MET crystal structures highlighting the torsional difference (relative to the 7-azaindole group) between the pyrazole group of **6** (blue carbons) compared to the pyrrolopyrrolinone group of **5** (white carbons). (c) Crystal structure of c-MET bound by compound **7**. See Figure S5 and Table S1 for further details.

without compromising potency. Indeed replacement of the pyrrolopyrrolinone group with a piperidine-substituted pyrazole (**6**) resulted in a significant reduction (over 1.5 log units) in logD (Table 2). The biochemical activity of **6** was also assessed, revealing an IC$_{50}$ of 48 nM for c-MET, a more than 10-fold improvement compared to compound **5** (Table 2). In order to investigate the structural basis of this increased

biochemical activity, we solved a crystal structure of compound **6** in complex with c-MET (Figure S5a). This structure revealed **6** to clearly bind to the folded P-loop conformation of the kinase and suggested that the increase in potency (compared to **5**) may be a result of a strong water bridge from the pyrazole group of **6** to residue D1164. In addition, the pyrazole group of **6** appears to be noticeably twisted (and therefore less energetically strained) compared to the bulkier pyrrolopyrro-linone group of **5** (Figure 3b), which may also contribute to the increased biochemical activity of **6** over **5**.

We next explored the benzyl group of **6** by searching our internal chemical library for analogues. Assessment of fluorine substitutions of the *ortho*- (**7**), *meta*- (**8**), and *para*- (**9**) positions of the benzyl ring revealed all positions to be amenable to substitution, with IC$_{50}$ values for **7–9** in the range of 44−137 nM (Table 2). Crystal structures were then determined for compounds **7–9** in complex with c-MET, with all three inhibitors shown to bind to the folded P-loop conformation of the kinase (Figures 3c and S5b,c). The cell activity of compounds **6–9** was then investigated using a cellular homogeneous time-resolved FRET (HTRF) assay. These experiments revealed compounds **6–9** to be able to effectively inhibit c-MET in a cellular setting, with IC$_{50}$ values in the single-digit μM range (Table 2).

As previous reports have linked the targeting of the folded P-loop conformation with favorable kinome selectivity,[14] we next sought to assess the kinome selectivity of our most active inhibitor (**7**). Compound **7** was screened at a concentration of 100 nM against a panel of 140 kinases, with 27 (~18%) inhibited by ≥60% (Table S2). While perhaps modest, this level of kinome selectivity offers promise for a series that is yet

to undergo extensive SAR exploration. Moreover, the low molecular weight (375 Da), coupled with the low lipophilicity of the inhibitors, provides ample scope for further optimization of this series.

The ability to target distinct conformational states of kinases, such as the DFG-out[7,9−11] and αC-helix-out conformations,[8,12,29] has proven to be of significant therapeutic value, yet the folded P-loop conformation has received far less attention. This is particularly true of c-MET, for which many chemotypes have been reported, yet few which bind to the folded P-loop form of the kinase.[4] We have reported here a series of fragments shown by crystallography to bind to the folded P-loop conformation of c-MET, with subsequent fragment merging and preliminary SAR exploration resulting in a series of inhibitors with nanomolar biochemical activity. Crystal structures confirmed all nanomolar inhibitors to bind to the folded P-loop conformation of c-MET via a novel type-I binding mode, with one compound (7) showing promising kinase selectivity and cell activity. This work increases our structural understanding of the folded P-loop conformation of c-MET and provides a sound structural basis for the further exploration of this conformational state with small molecule inhibitors.

◼ ASSOCIATED CONTENT

ⓢ Supporting Information

The Supporting Information is available free of charge at https://pubs.acs.org/doi/10.1021/acsmedchemlett.0c00392.

> Additional figures and detailed description of methods concerning protein expression and purification, NMR, SPR, biochemical and cellular assays, kinase selectivity, X-ray crystallography, and chemistry (PDF)

◼ AUTHOR INFORMATION

Corresponding Author

Gavin W. Collie − *Discovery Sciences, R&D, AstraZeneca, Cambridge, United Kingdom;* ⓘ orcid.org/0000-0002-0406-922X; Email: gavin.collie@astrazeneca.com

Authors

Iacovos N. Michaelides − *Discovery Sciences, R&D, AstraZeneca, Cambridge, United Kingdom*

Kevin Embrey − *Discovery Sciences, R&D, AstraZeneca, Cambridge, United Kingdom*

Christopher J. Stubbs − *Discovery Sciences, R&D, AstraZeneca, Cambridge, United Kingdom*

Ulf Börjesson − *Discovery Sciences, R&D, AstraZeneca, Gothenburg, Sweden*

Ian L. Dale − *Discovery Sciences, R&D, AstraZeneca, Cambridge, United Kingdom*

Arjan Snijder − *Discovery Sciences, R&D, AstraZeneca, Gothenburg, Sweden*

Louise Barlind − *Discovery Sciences, R&D, AstraZeneca, Gothenburg, Sweden*

Kun Song − *Oncology, R&D, AstraZeneca, Boston, United States*

Puneet Khurana − *Discovery Sciences, R&D, AstraZeneca, Cambridge, United Kingdom*

Christopher Phillips − *Discovery Sciences, R&D, AstraZeneca, Cambridge, United Kingdom*

R. Ian Storer − *Discovery Sciences, R&D, AstraZeneca, Cambridge, United Kingdom*

Complete contact information is available at:
https://pubs.acs.org/10.1021/acsmedchemlett.0c00392

◼ ABBREVIATIONS

A-loop, activation loop; c-MET, mesenchymal-epithelial transition factor; HTRF, homogeneous time-resolved FRET; FRET, Förster resonance energy transfer; P-loop, phosphate-binding loop; SAR, structure-activity relationship; SPR, surface plasmon resonance

◼ REFERENCES

(1) The c-MET P-loop is defined here as spanning residues 1084−1092, with the following sequence: IGRGHFGCV.

(2) Wang, W.; Marimuthu, A.; Tsai, J.; Kumar, A.; Krupka, H. I.; Zhang, C.; Powell, B.; Suzuki, Y.; Nguyen, H.; Tabrizizad, M.; Luu, C.; West, B. L. Structural characterization of autoinhibited c-Met kinase produced by coexpression in bacteria with phosphatase. *Proc. Natl. Acad. Sci. U. S. A.* **2006**, *103*, 3563−3568.

(3) Buchanan, S. G.; Hendle, J.; Lee, P. S.; Smith, C. R.; Bounaud, P. Y.; Jessen, K. A.; Tang, C. M.; Huser, N. H.; Felce, J. D.; Froning, K. J.; Peterman, M. C.; Aubol, B. E.; Gessert, S. F.; Sauder, J. M.; Schwinn, K. D.; Russell, M.; Rooney, I. A.; Adams, J.; Leon, B. C.; Do, T. H.; Blaney, J. M.; Sprengeler, P. A.; Thompson, D. A.; Smyth, L.; Pelletier, L. A.; Atwell, S.; Holme, K.; Wasserman, S. R.; Emtage, S.; Burley, S. K.; Reich, S. H. SGX523 is an exquisitely selective, ATP-competitive inhibitor of the MET receptor tyrosine kinase with antitumor activity in vivo. *Mol. Cancer Ther.* **2009**, *8*, 3181−3190.

(4) D'Angelo, N. D.; Bellon, S. F.; Booker, S. K.; Cheng, Y.; Coxon, A.; Dominguez, C.; Fellows, I.; Hoffman, D.; Hungate, R.; Kaplan-Lefko, P.; Lee, M. R.; Li, C.; Liu, L.; Rainbeau, E.; Reider, P. J.; Rex, K.; Siegmund, A.; Sun, Y.; Tasker, A. S.; Xi, N.; Xu, S.; Yang, Y.; Zhang, Y.; Burgess, T. L.; Dussault, I.; Kim, T. S. Design, synthesis, and biological evaluation of potent c-Met inhibitors. *J. Med. Chem.* **2008**, *51*, 5766−5779.

(5) Lightfoot, H. L.; Goldberg, F. W.; Sedelmeier, J. Evolution of Small Molecule Kinase Drugs. *ACS Med. Chem. Lett.* **2019**, *10*, 153−160.

(6) Roskoski, R., Jr. Properties of FDA-approved small molecule protein kinase inhibitors. *Pharmacol. Res.* **2019**, *144*, 19−50.

(7) Dietrich, J.; Hulme, C.; Hurley, L. H. The design, synthesis, and evaluation of 8 hybrid DFG-out allosteric kinase inhibitors: a structural analysis of the binding interactions of Gleevec, Nexavar, and BIRB-796. *Bioorg. Med. Chem.* **2010**, *18*, 5738−5748.

(8) Millan, D. S.; Bunnage, M. E.; Burrows, J. L.; Butcher, K. J.; Dodd, P. G.; Evans, T. J.; Fairman, D. A.; Hughes, S. J.; Kilty, I. C.; Lemaitre, A.; Lewthwaite, R. A.; Mahnke, A.; Mathias, J. P.; Philip, J.; Smith, R. T.; Stefaniak, M. H.; Yeadon, M.; Phillips, C. Design and

synthesis of inhaled p38 inhibitors for the treatment of chronic obstructive pulmonary disease. *J. Med. Chem.* **2011**, *54*, 7797−7814.

(9) Nagar, B.; Bornmann, W. G.; Pellicena, P.; Schindler, T.; Veach, D. R.; Miller, W. T.; Clarkson, B.; Kuriyan, J. Crystal structures of the kinase domain of c-Abl in complex with the small molecule inhibitors PD173955 and imatinib (STI-571). *Cancer Res.* **2002**, *62*, 4236−4243.

(10) Schindler, T.; Bornmann, W.; Pellicena, P.; Miller, W. T.; Clarkson, B.; Kuriyan, J. Structural mechanism for STI-571 inhibition of abelson tyrosine kinase. *Science* **2000**, *289*, 1938−1942.

(11) Vijayan, R. S.; He, P.; Modi, V.; Duong-Ly, K. C.; Ma, H.; Peterson, J. R.; Dunbrack, R. L., Jr.; Levy, R. M. Conformational analysis of the DFG-out kinase motif and biochemical profiling of structurally validated type II inhibitors. *J. Med. Chem.* **2015**, *58*, 466−479.

(12) Wood, E. R.; Truesdale, A. T.; McDonald, O. B.; Yuan, D.; Hassell, A.; Dickerson, S. H.; Ellis, B.; Pennisi, C.; Horne, E.; Lackey, K.; Alligood, K. J.; Rusnak, D. W.; Gilmer, T. M.; Shewchuk, L. A unique structure for epidermal growth factor receptor bound to GW572016 (Lapatinib): relationships among protein conformation, inhibitor off-rate, and receptor activity in tumor cells. *Cancer Res.* **2004**, *64*, 6652−6659.

(13) Counago, R. M.; Allerston, C. K.; Savitsky, P.; Azevedo, H.; Godoi, P. H.; Wells, C. I.; Mascarello, A.; de Souza Gama, F. H.; Massirer, K. B.; Zuercher, W. J.; Guimaraes, C. R. W.; Gileadi, O. Structural characterization of human Vaccinia-Related Kinases (VRK) bound to small-molecule inhibitors identifies different P-loop conformations. *Sci. Rep.* **2017**, *7*, 7501.

(14) Guimaraes, C. R.; Rai, B. K.; Munchhof, M. J.; Liu, S.; Wang, J.; Bhattacharya, S. K.; Buckbinder, L. Understanding the impact of the P-loop conformation on kinase selectivity. *J. Chem. Inf. Model.* **2011**, *51*, 1199−1204.

(15) Patel, R. Y.; Doerksen, R. J. Protein kinase-inhibitor database: structural variability of and inhibitor interactions with the protein kinase P-loop. *J. Proteome Res.* **2010**, *9*, 4433−4442.

(16) Hari, S. B.; Perera, B. G.; Ranjitkar, P.; Seeliger, M. A.; Maly, D. J. Conformation-selective inhibitors reveal differences in the activation and phosphate-binding loops of the tyrosine kinases Abl and Src. *ACS Chem. Biol.* **2013**, *8*, 2734−2743.

(17) Zhang, Y.; Xia, M.; Jin, K.; Wang, S.; Wei, H.; Fan, C.; Wu, Y.; Li, X.; Li, X.; Li, G.; Zeng, Z.; Xiong, W. Function of the c-Met receptor tyrosine kinase in carcinogenesis and associated therapeutic opportunities. *Mol. Cancer* **2018**, *17*, 45.

(18) Parikh, P. K.; Ghate, M. D. Recent advances in the discovery of small molecule c-Met Kinase inhibitors. *Eur. J. Med. Chem.* **2018**, *143*, 1103−1138.

(19) Cui, J. J.; Tran-Dube, M.; Shen, H.; Nambu, M.; Kung, P. P.; Pairish, M.; Jia, L.; Meng, J.; Funk, L.; Botrous, I.; McTigue, M.; Grodsky, N.; Ryan, K.; Padrique, E.; Alton, G.; Timofeevski, S.; Yamazaki, S.; Li, Q.; Zou, H.; Christensen, J.; Mroczkowski, B.; Bender, S.; Kania, R. S.; Edwards, M. P. Structure based drug design of crizotinib (PF-02341066), a potent and selective dual inhibitor of mesenchymal-epithelial transition factor (c-MET) kinase and anaplastic lymphoma kinase (ALK). *J. Med. Chem.* **2011**, *54*, 6342−6363.

(20) Dong, H. J.; Li, P.; Wu, C. L.; Zhou, X. Y.; Lu, H. J.; Zhou, T. Response and acquired resistance to crizotinib in Chinese patients with lung adenocarcinomas harboring MET Exon 14 splicing alternations. *Lung Cancer* **2016**, *102*, 118−121.

(21) Heist, R. S.; Sequist, L. V.; Borger, D.; Gainor, J. F.; Arellano, R. S.; Le, L. P.; Dias-Santagata, D.; Clark, J. W.; Engelman, J. A.; Shaw, A. T.; Iafrate, A. J. Acquired Resistance to Crizotinib in NSCLC with MET Exon 14 Skipping. *J. Thorac. Oncol.* **2016**, *11*, 1242−1245.

(22) Kang, J.; Chen, H. J.; Wang, Z.; Liu, J.; Li, B.; Zhang, T.; Yang, Z.; Wu, Y. L.; Yang, J. J. Osimertinib and Cabozantinib Combinatorial Therapy in an EGFR-Mutant Lung Adenocarcinoma Patient with Multiple MET Secondary-Site Mutations after Resistance to Crizotinib. *J. Thorac. Oncol.* **2018**, *13*, e49−e53.

(23) Ou, S. I.; Young, L.; Schrock, A. B.; Johnson, A.; Klempner, S. J.; Zhu, V. W.; Miller, V. A.; Ali, S. M. Emergence of Preexisting MET Y1230C Mutation as a Resistance Mechanism to Crizotinib in NSCLC with MET Exon 14 Skipping. *J. Thorac. Oncol.* **2017**, *12*, 137−140.

(24) Schrock, A. B.; Lai, A.; Ali, S. M.; Miller, V. A.; Raez, L. E. Mutation of MET Y1230 as an Acquired Mechanism of Crizotinib Resistance in NSCLC with MET Exon 14 Skipping. *J. Thorac. Oncol.* **2017**, *12*, e89−e90.

(25) Reungwetwattana, T.; Liang, Y.; Zhu, V.; Ou, S. I. The race to target MET exon 14 skipping alterations in non-small cell lung cancer: The Why, the How, the Who, the Unknown, and the Inevitable. *Lung Cancer* **2017**, *103*, 27−37.

(26) Further details of the crystallographic methods used in this work, including the development of a soakable system for the P-loop conformation, can be found in Figure S1 in the Supporting Information.

(27) ADP-Glo biochemical enzyme inhibition assay. Full details can be found in the Supporting Information.

(28) Compound **5** was also assessed by SPR, giving a K_D of 5.3 μM for c-MET.

(29) Palmieri, L.; Rastelli, G. alphaC helix displacement as a general approach for allosteric modulation of protein kinases. *Drug Discovery Today* **2013**, *18*, 407−414.

■ NOTE ADDED AFTER ASAP PUBLICATION

This paper was originally published ASAP on December 8, 2020. A revised Supporting Information file was uploaded, and the paper reposted on December 10, 2020.